Journal of Computational Acoustics, Vol. 6, No. 4 (1998) 421–434

ACOUSTIC SCATTERING BY TWO SUBMERGED SPHERICAL SHELLS: NUMERICAL VALIDATION

GORDON C. EVERSTINE and GUILLERMO C. GAUNAURD
Naval Surface Warface Center, Carderock Division
Bethesda, MD 20817-5700, USA

HANSON HUANG
Consultant, Bowie, MD 20715, USA

Received 1 April 1997
Revised 28 May 1998

We validate, using a coupled finite element/boundary element computer code, a recently-developed[1] series solution for the structural acoustics problem of scattering from two submerged spherical elastic shells. Although the general purpose computational tools for acoustic scattering have never been restricted to single scatterers, the availability of the series solution provides, for the first time, the mutual validation of both exact and numerical approaches for a multiple elastic scatterer problem. The excellent agreement between the two solutions presented thus allows this problem to be added to the short list of existing benchmark structural acoustics problems possessing an analytic solution. For the purposes of this comparison, the direction of incidence is taken as parallel with the axis joining the two shells. The numerical solution uses the NASHUA code, which couples a finite element shell model of the two shells with a boundary element model of the surrounding fluid. The exact solution is found by expanding in terms of classical modal series and uses the addition theorem for the spherical wave functions. The exact solution requires coupling coefficients that are expressed in terms of sums of products of Wigner 3-j symbols (or Clebsch-Gordan coefficients).

1. Introduction

Two important problems in numerical structural acoustics are: (1) the calculation of the acoustic pressure field radiated by a general submerged three-dimensional elastic structure subjected to internal time-harmonic loads, and (2) the calculation of the far-field acoustic pressure scattered by an elastic structure subjected to an incident, time-harmonic wavetrain. The most common, as well as the most accurate, general approach for solving these problems is to couple a finite element model of the structure with a boundary element model of the surrounding fluid.[2–5]

Computer program validation has always posed a problem to program developers, but validation of structural acoustics codes is particularly challenging, since the only coupled

fluid-structure problems possessing analytic solutions involve Cartesian, spherical, or cylindrical geometry. Series solutions exist for submerged spherical shells and solid bodies subjected to uniform and non-uniform mechanical loads and external incident pressure loads (acoustic scattering).[6,7] Series solutions also exist for scattering from a submerged fluid-filled spherical shell[7,8] and for a submerged spherical shell containing a two-degree-of-freedom elastic system attached inside.[9,10] Although the solution of such problems is a necessary step in the validation of a numerical procedure, more complicated problems are also needed, including problems with multiple scatterers.

A recent paper[1] presented a series solution for the problem of acoustic scattering from two submerged spherical elastic shells. This problem is of interest both for the physics which are revealed and for its use as a potential additional benchmark problem for further validation of structural acoustics computer codes. Previously, there have been no known analytic solutions involving multiple elastic scatterers.

In this paper, we will compare solutions to this problem obtained by both large-scale computation and the exact series solution. Harmonic excitation for non-dimensional frequencies up to $ka = 20$ will be presented. For completeness, both solution approaches will also be briefly summarized.

2. Problem Description

Two spherical elastic shells, one above the other, have centers distance d apart and are immersed in an acoustic fluid of mass density ρ and sound speed c. We denote the outer and inner radii of the lower and upper shells as a, b and a', b', respectively (Fig. 1). Thus, the thickness of the shells two are $h = a - b$ and $h' = a' - b'$. The mass densities and the compressional and shear wavespeeds in the shells are ρ_s, c_d, c_s and ρ'_s, c'_d, and c'_s, respectively. From these quantities, the Young's moduli E, E' and the Poisson's ratios ν, ν' can be calculated from the formulae

$$E = \rho c_s^2 \frac{3c_d^2 - 4c_s^2}{c_d^2 - c_s^2}, \quad \nu = \frac{c_d^2 - 2c_s^2}{2(c_d^2 - c_s^2)}, \tag{2.1}$$

and analogously for E' and ν'. The mass densities and sound speeds of their internal fluids are ρ_i, c_i and ρ'_i, c'_i, respectively. Two spherical coordinate systems (r, θ, ϕ) and (r', θ', ϕ') are located at the centers O and O' of the two shells. The azimuthal coordinate ϕ is common to both systems and is not shown in Fig. 1. An acoustic plane wave is incident on the shells so that its propagation vector forms an angle α with the line $\overline{OO'}$. The shells interact with the fluid and with each other in an elasto-acoustic fashion. As the incident wave impinges upon them, a multiple-scattering process of re-reflections and re-bounces is initiated. The scattered pressure field from either shell acts as a secondary incident wave on the other. This secondary effect is followed by tertiary, quaternary, etc., incidences, until the interaction vanishes. The mathematical formulation given below will account exactly for this multiple re-scattering process.

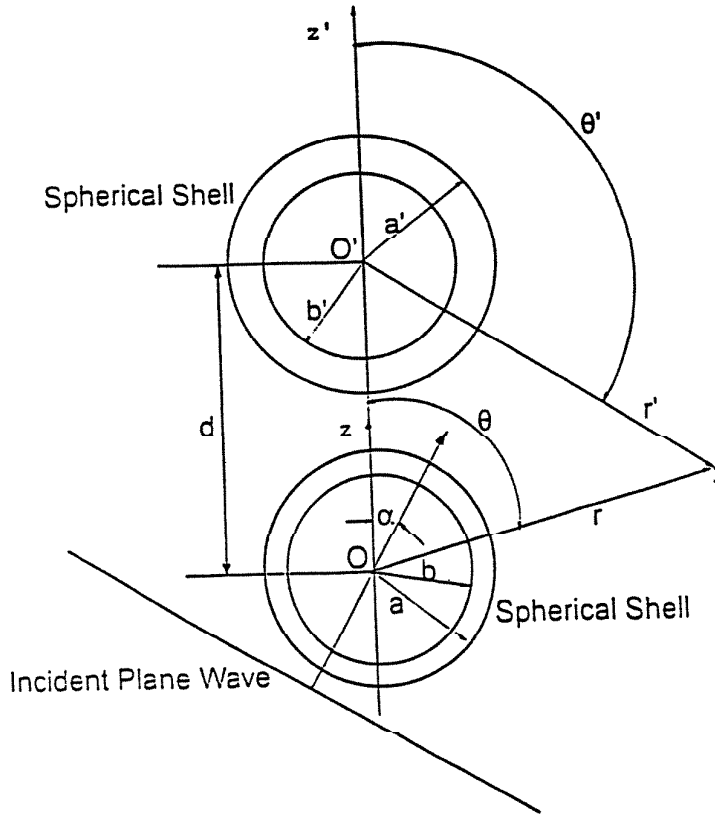

Fig. 1. Geometry of the scattering problem. Two spherical elastic shells insonified by a plane sound wave.

3. The Analytic Solution

The formulation below is similar to that used earlier,[1] in which the motions of the shells are described by the standard bending shell theory and the various boundary conditions associated with them. The equations of three-dimensional elasticity could alternatively be used to describe the shell motions. However, to describe the scattering by two shells, it is necessary to have the analytic expression for the scattering from a single shell. This expression has been used often in the past,[9,11–13] and is assumed to be known here.

It is convenient to define first the following dimensionless variables:

$$\begin{gathered} R = r/a,\ R' = r'/a,\ D = d/a,\ \Omega = \omega a/c = ka,\ \Omega_i = (c/c_i)\Omega\,, \\ \Omega_i' = (c/c_i')\Omega,\ \Pi = p/(\rho c^2),\ \Pi_i = p_i/(\rho c^2),\ \Pi_i' = p_i'/(\rho c^2)\,, \\ \xi = a'/a,\ M = \rho a/(\rho_s h),\ M' = \rho a'/(\rho_s' h'),\ \beta^2 = h^2/(12a^2)\,, \\ \beta'^2 = h'^2/(12a'^2),\ C = E/[\rho_s c^2(1-\nu)],\ C' = E'/[\rho_s' c^2(1-\nu')]\,. \end{gathered} \tag{3.1}$$

Here, p, p_i, and p_i' are the pressure fields in the outer fluid, and the pressure fields inside the lower and upper shells, respectively. Analogously, Π, Π_i, and Π_i' are the non-dimensional

pressure fields satisfying the Helmholtz equation in their respective domains. The circular frequency of the incident wave is ω, and k is its wavenumber.

The incident plane wave is given in both coordinate systems by

$$\begin{aligned}\Pi^{\text{inc}} &= e^{i\Omega R(\cos\theta\cos\alpha+\sin\theta\sin\alpha\cos\phi)}\\ &= e^{i\Omega R'(\cos\theta'\cos\alpha+\sin\theta'\sin\alpha\cos\phi)}e^{i\Omega D\cos\alpha}\,.\end{aligned} \tag{3.2}$$

The spherical wave function expansion of the incident wave in both systems is

$$\begin{aligned}\Pi^{\text{inc}} &= 2\sum_{n=0}^{\infty}\sum_{m=0}^{n} i^n\frac{2-\delta_{0m}}{N_{mn}}j_n(\Omega R)P_n^m(\cos\theta)P_n^m(\cos\alpha)e^{im\phi}\\ &= e^{i\Omega D\cos\alpha}2\sum_{n=0}^{\infty}\sum_{m=0}^{n} i^n\frac{2-\delta_{0m}}{N_{mn}}j_n(\Omega R')P_n^m(\cos\theta')P_n^m(\cos\alpha)e^{im\phi}\,,\end{aligned} \tag{3.3}$$

where j_n is the spherical Bessel function of the first kind, P_n^m is the associated Legendre function, δ_{ij} is the Kronecker delta, and

$$N_{nm} = [2(n+m)!]/[(2n+1)(n-m)!]\,. \tag{3.4}$$

The external pressure field scattered by both shells in the presence of each other is

$$\begin{aligned}\Pi^{\text{sca}} = \sum_{n=0}^{\infty}\sum_{m=0}^{n}&[B_{mn}h_n(\Omega R)P_n^m(\cos\theta)\\ &+ b_{mn}h_n(\Omega R')P_n^m(\cos\theta')]e^{im\phi}\,,\end{aligned} \tag{3.5}$$

where h_n is the spherical Hankel function of the first kind, and the coupling coefficients B_{mn} and b_{mn} are determined from the boundary conditions. It is the coupling of the coefficients which accounts for all levels of multiple scattering. The total pressure field in the outer fluid in the system at O is

$$\begin{aligned}\Pi &= \Pi^{\text{inc}} + \Pi^{\text{sca}}\\ &= 2\sum_{n=0}^{\infty}\sum_{m=0}^{n} i^n\frac{2-\delta_{0m}}{N_{mn}}j_n(\Omega)P_n^m(\cos\theta)P_n^m(\cos\alpha)e^{im\phi}\\ &\quad+\sum_{n=0}^{\infty}\sum_{m=0}^{n} B_{mn}h_n(\Omega R)P_n^m(\cos\theta)e^{im\phi}\\ &\quad+\sum_{q=0}^{\infty}\sum_{m=0}^{q} b_{qm}\sum_{n=m}^{\infty} Q_{mnmq}(D,\pi)j_n(\Omega R)P_n^m(\cos\theta)e^{im\phi}\,.\end{aligned} \tag{3.6}$$

The same total pressure field expressed in the primed system (r', θ', ϕ') is

$$\begin{aligned}\Pi = {} & 2e^{i\Omega D\cos\theta}\sum_{n=0}^{\infty}\sum_{m=0}^{n} i^n \frac{2-\delta_{0m}}{N_{mn}} j_n(\Omega R')P_n^m(\cos\theta')P_n^m(\cos\alpha)e^{im\phi} \\ & + \sum_{n=0}^{\infty}\sum_{m=0}^{n} b_{mn}h_n(\Omega R')P_n^m(\cos\theta')e^{im\phi} \\ & + \sum_{q=0}^{\infty}\sum_{m=0}^{q} B_{mq}\sum_{n=m}^{\infty} Q_{mnmq}(D,0)j_n(\Omega R')P_n^m(\cos\theta')e^{im\phi}\,. \end{aligned} \tag{3.7}$$

We have used the addition theorem for the spherical wave functions[14] to have Eq. (3.6) [or Eq. (3.7)] completely expressed in the unprimed (or primed) coordinate system. To this effect, we have used

$$Q_{mnmq}(D,\pi) = \frac{2i^{n-q}}{N_{mn}}\sum_{\sigma=|n-q|}^{n+q} i^\sigma(-1)^\sigma b_\sigma^{qmnm}h_\sigma(\Omega D)\,, \tag{3.8}$$

$$Q_{mnmq}(D,0) = \frac{2i^{n-q}}{N_{mn}}\sum_{\sigma=|n-q|}^{n+q} i^\sigma b_\sigma^{qmnm}h_\sigma(\Omega D)\,. \tag{3.9}$$

These last two expressions differ only by the factor $(-1)^\sigma$. The b_σ are given by

$$b_\sigma^{qmnm} = (-1)^m(2\sigma+1)\sqrt{\frac{(q+m)!(n+m)!}{(q-m)!(n-m)!}}\begin{bmatrix} q & n & \vdots & \sigma \\ 0 & 0 & \vdots & 0\end{bmatrix}\begin{bmatrix} q & n & \vdots & \sigma \\ m & -m & \vdots & 0\end{bmatrix} \tag{3.10}$$

in terms of the Wigner 3-j symbols defined elsewhere,[15,16] or

$$b_\sigma^{qmnm} = (-1)^m\sqrt{\frac{(q+m)!(n+m)!}{(q-m)!(n-m)!}}(q,n,0,0|\sigma,0)(q,n,m,-m|\sigma,0) \tag{3.11}$$

in terms of the Clebsch-Gordan coefficients.[14,17]

At the shell boundaries, the displacements and normal stresses must be continuous, and the tangential stresses must vanish, since all the fluids considered here are inviscid. Application of these boundary conditions yields the following coupled system of equations:

$$\begin{aligned} B_{mn} + \left[\sum_{q=m}^{\infty} b_{mq}Q_{mnmq}(D,\pi)\right]X_n(\Omega) &= -2i^n\frac{2-\delta_{0m}}{N_{mn}}P_n^m(\cos\alpha)X_n(\Omega) \\ b_{mn} + \left[\sum_{q=m}^{\infty} B_{mq}Q_{mnmq}(D,0)\right]X_n'(\Omega) &= -2i^n\frac{2-\delta_{0m}}{N_{mn}}P_n^m(\cos\alpha)X_n'(\Omega)e^{i\Omega D\cos\alpha}\,, \end{aligned} \tag{3.12}$$

where the $X_n(\Omega)$ are the scattering coefficients for a single shell.

Two choices for these coefficients are available at this point. If we select the bending shell theory to describe the motions of the shells,[1] these coefficients are given by

$$X_n(\Omega) = \frac{\Gamma_n j_n'(\Omega) + \Omega j_n(\Omega)}{\Gamma_n h_n'(\Omega) + \Omega h_n(\Omega)}, \tag{3.13}$$

where

$$\Gamma_n = \frac{\Omega^4 - (A_n + C_n)\Omega^2 + (A_n C_n - B_n D_n)}{M(C_n - \Omega^2)}, \tag{3.14}$$

$$A_n = C^2 \left[2 + \beta^2 n(n+1)\frac{n(n+1) - (1-\nu)}{1+\nu}\right], \tag{3.15}$$

$$B_n = C^2 n(n+1)\left[1 + \beta^2 \frac{n(n+1) - (1-\nu)}{1+\nu}\right], \tag{3.16}$$

$$C_n = C^2(1+\beta^2)\frac{n(n+1) - (1-\nu)}{1+\nu}, \tag{3.17}$$

$$D_n = \frac{B_n}{n(n+1)}, \tag{3.18}$$

and analogously for the $X_n'(\Omega)$ for the upper shell. For the shells studied here, this formulation is valid[9] up to $ka \approx 25$.

If the motions of the shells are described by the exact three-dimensional theory of elasticity, then the set of scattering coefficients $X_n(\Omega)$ for the single shell is the first unknown solution of the 6×6 system of linear algebraic equations

$$\hat{D} X_n(\Omega) = -A^*, \tag{3.19}$$

where the coefficient matrix $\hat{D}$ and the right-hand side column vector A^* are defined elsewhere.[12] $X_n'(\Omega)$ is solved similarly, except that the properties of the upper shell (i.e. a', b', ρ_s', c_d', c_s', ...) are used instead of those of the lower shell. These two quantities contain all the three-dimensional elastodynamic effects. This formulation is valid for all ka ranges.

In the frequency range to be used here, and for the shell thicknesses and materials of interest here, the two formulations give the same results. We therefore choose to use the simpler bending shell theory for the calculation of results.

For each m, Eq. (3.12) can be arranged in the matrix form

$$\begin{aligned} B + \Lambda b &= S \\ b + AB &= S' e^{i\Omega D \cos\alpha}, \end{aligned} \tag{3.20}$$

where the vectors B and b represent B_{mn} and b_{mn}, and Λ, A, S, and S' have elements

$$\Lambda_{kj} = Q_{mkmj}(D, \pi) X_j(\Omega) \tag{3.21}$$

$$A_{kj} = Q_{mkmj}(D, 0) X_j'(\Omega) \tag{3.22}$$

$$S_j = -2i^j \frac{2-\delta_{m0}}{N_{mj}} X_j(\Omega) P_j^m(\cos\alpha) \tag{3.23}$$

$$S'_j = -2i^j \frac{2-\delta_{m0}}{N_{mj}} X'_j(\Omega) P_j^m(\cos\alpha)\,, \tag{3.24}$$

where the indices k and j range from m to N, and $i = \sqrt{-1}$. Here, Λ and A are $(N+1-m) \times (N+1-m)$ complex matrices, and S_j and S'_j are $(N+1-m)$ complex vectors for each m.

For large R, we can use the asymptotic relation[18]

$$h_n(\Omega R) \to i^{-(n+1)} e^{i\Omega R}/(\Omega R)\,, \tag{3.25}$$

and then the far-field pressure scattered by the pair of shells becomes

$$\Pi^{sca}(R,\theta,\phi,\Omega) = [e^{i\Omega R}/(\Omega R)] \sum_{n=0}^{\infty} \sum_{m=0}^{n} i^{-(n+1)} [B_{mn} P_n^m(\cos\theta) + b_{mn}(R/R') e^{i\Omega(R'-R)} P_n^m(\cos\theta')] e^{im\phi}\,. \tag{3.26}$$

The primed coordinates can be expressed in terms of the unprimed set by

$$R' = \sqrt{R^2 + D^2 - 2RD\cos\theta} \tag{3.27}$$

$$\theta' = \begin{cases} \sin^{-1}\left(\dfrac{R}{R'}\sin\theta\right), & 0 \le \theta \le \pi/2 \\ \pi - \sin^{-1}\left(\dfrac{R}{R'}\sin\theta\right), & \pi/2 \le \theta \le 3\pi/2 \\ 2\pi - \sin^{-1}\left(\dfrac{R}{R'}\sin\theta\right), & 3\pi/2 \le \theta \le 2\pi\,. \end{cases} \tag{3.28}$$

Finally, the form function is defined as the absolute value of

$$f_\infty(R,\theta,\phi,\Omega) = 2Re^{-i\Omega R}\Pi^{\text{sca}}(R,\theta,\phi,\Omega)\,. \tag{3.29}$$

Thus, the form function is

$$|f_\infty(R,\theta,\phi,\Omega)| = (2/\Omega) \left| \sum_{n=0}^{\infty} \sum_{m=0}^{n} (-i)^{n+1} e^{im\phi} \left[B_{mn} P_n^m(\cos\theta) + \frac{b_{mn}}{\sqrt{1+(D/R)^2 - 2(D/R)\cos\theta}} \times e^{i\Omega R(\sqrt{1+(D/R)^2-2(D/R)\cos\theta}-1)}] P_n^m(\cos\theta') \right|\,, \tag{3.30}$$

where θ' is given in Eq. (3.28), and the coupling coefficients B_{mn} and b_{mn} are the solutions of the coupled transcendental system, Eq. (3.20), which is solved by Gauss-Seidel iteration.

In the present work, the particular incidence direction of interest is the endfire ($\alpha = 0$) direction. In this case, one shell eclipses the other, and it is the most physically interesting situation.

4. The Numerical Solution

The numerical solution of this problem is the coupling of a finite element model of the structure with a boundary element model of the exterior fluid,[5] as summarized in this section.

Consider a submerged three-dimensional elastic structure subjected to either internal time-harmonic mechanical loads or an external time-harmonic incident wavetrain. If the structure is modeled with finite elements, the resulting matrix equation of motion can be written as

$$Zv = F - GAp\,, \tag{4.1}$$

where matrix Z (of dimension $s \times s$) is the structural impedance, vector v ($s \times r$) is the complex velocity amplitude for all structural DOF (wet and dry) using the coordinate systems selected by the user, vector F ($s \times r$) is the complex amplitude of the mechanical forces applied to the structure, matrix G ($s \times f$) is the rectangular transformation of direction cosines to transform a vector of outward normal forces at the wet points to a vector of forces at all points in the coordinate systems selected by the user, matrix A ($f \times f$) is the diagonal area matrix for the wet surface, and vector p ($f \times r$) is the complex amplitude of total pressures (incident + scattered) applied at the wet grid points. In Eq. (4.1), the time dependence $\exp(i\omega t)$ has been suppressed. In the above dimensions, s denotes the total number of independent structural DOF (wet and dry), f denotes the number of fluid DOF (equal to the number of wet structural points), and r denotes the number of load cases. A load case consists of a particular mechanical excitation or an external incident pressure from a particular direction. In general, the surface areas, the normals, and the transformation matrix G are obtained from the finite element calculation of the load vector resulting from an outwardly directly static unit pressure load on the structure's wet surface.

In Eq. (4.1), the structural impedance matrix Z, which converts velocity to force, is given by

$$Z = (-\omega^2 M + i\omega B + K)/(i\omega)\,, \tag{4.2}$$

where M, B, and K are the structural mass, viscous damping, and stiffness matrices, respectively, and ω is the circular frequency of excitation. For structures with a non-zero loss factor, K is complex. In addition, K can include the stiffening effects of hydrostatic pressure.[19] A standard finite element model of the structure supplies the matrices K, M, and B.

For the exterior fluid domain, the fluid pressure p satisfies the Helmholtz equation

$$\nabla^2 p + k^2 p = 0\,, \tag{4.3}$$

where $k = \omega/c$ is the acoustic wavenumber and c is the fluid sound speed. This differential

equation for the exterior domain can alternatively be written in integral form on the fluid-structure interface:

$$\frac{p(\mathbf{x}')}{2} - \oint_S p(\mathbf{x}) \frac{e^{-ikr}}{4\pi r} \left(ik + \frac{1}{r} \right) \cos\psi dS = i\omega\rho \oint_S v_n(\mathbf{x}) \frac{e^{-ikr}}{4\pi r} dS + p_I, \ \mathbf{x}' \text{ on } S\,, \tag{4.4}$$

where p denotes total fluid pressure (incident + scattered) on the surface S (Fig. 2), $\mathbf{x}$ is the position vector for a typical point P_j on S, $\mathbf{x}'$ is the position vector for the point P_i on the surface, the vector $\mathbf{r} = \mathbf{x}' - \mathbf{x}$, $\mathbf{n}$ is the unit outward normal at P_j, ρ is the fluid mass density, v_n is the outward normal velocity on S, ψ is the angle between $\mathbf{n}$ and $\mathbf{r}$, and p_I is the incident free-field pressure. We denote the lengths of the vectors $\mathbf{x}$, $\mathbf{x}'$, and $\mathbf{r}$ by x, x', and r, respectively.

This integral equation relates the pressure p and normal velocity v_n on S. If the integrals in Eq. (4.4) are discretized for numerical computation,[5] we obtain the boundary element matrix equation for the exterior fluid

$$Ep = Cv_n + p_I\,, \tag{4.5}$$

where vector p (of dimension $f \times r$) is the vector of complex amplitudes of the pressure on the structure's wet surface; matrices E and C (both $f \times f$) are fully-populated, complex, non-symmetric, and frequency-dependent; and vector p_I ($f \times r$) is the complex amplitude of the incident pressure vector. The number of unknowns in this system is f, the number of wet points on the fluid-structure interface.

The normal velocity vector v_n is related to the full velocity vector v by the same rectangular transformation matrix G:

$$v_n = G^T v\,, \tag{4.6}$$

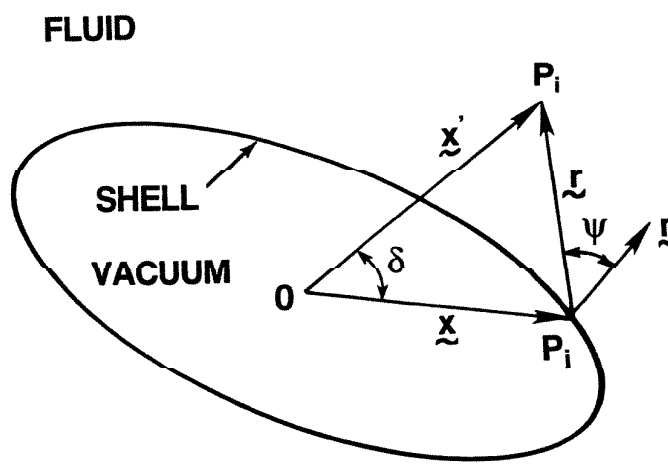

Fig. 2. Notation and parameters used in the derivation of the Helmholtz integral equation.

where T denotes the matrix transpose. If velocities v and v_n are eliminated from Eqs. (32), (36) and (37), the resulting equation for the coupled fluid-structure system is

$$(E + CG^T Z^{-1} GA)p = CG^T Z^{-1} F + p_I \,. \tag{4.7}$$

This equation can be solved for the vector p of surface pressures, since the rest of the equation depends only on the geometry, the material properties and the frequency. Since the two right-hand side terms in Eq. (4.7) correspond to mechanical and incident loadings, only one of the two terms would ordinarily be present for a given case. For the scattering problem of interest here, only the incident pressure p_I is present on the right-hand side of Eq. (4.7).

The velocity vector v for all structural DOF is recovered by solving Eq. (4.1) for v, and the surface normal velocity vector v_n is recovered by substituting this solution for v into Eq. (4.6).

With the solution for the pressures and velocities on the surface, the pressures radiated or scattered at points $\mathbf{x}'$ in the exterior domain can be obtained by integrating the exterior form of the Helmholtz integral equation (expressed here in asymptotic far-field form):

$$p(\mathbf{x}') = \frac{ike^{-ikx'}}{4\pi x'} \oint_S [\rho c v_n(\mathbf{x}) + p(\mathbf{x}) \cos\psi] e^{ikx\cos\delta} dS, \ \mathbf{x}' \text{ in } E, \ x' \gg \hat{d}\,, \tag{4.8}$$

where $\hat{d}$ is a characteristic dimension of the structure, and δ is the angle between the vectors $\mathbf{x}$ and $\mathbf{x}'$ (Fig. 2).

The above formulation has been implemented in the NASHUA procedure,[5] which couples a boundary element fluid model with a NASTRAN finite element structural model. CSA/NASTRAN[20] was used for the present calculations. The solution procedure thus uses CSA/NASTRAN to generate the matrices K, M, B, and F and to generate sufficient geometry information so that the matrices E, C, G, A, and p_I can be computed by a separate program. Then, CSA/NASTRAN's matrix routines are used to form the matrices appearing in Eq. (4.7), which is solved for the surface pressure p using the block solver OCSOLV.[21] Next, matrix operations are used to recover the surface normal velocities v_n and the vector v of velocities at all structural DOF. This step completes the surface solution. Finally, far-field radiated or scattered pressures are obtained by integrating the surface pressures and normal velocities using Eq. (4.8).

5. Results and Discussion

Here, we compare the exact (analytic) solution for the acoustic scattering from two identical spherical shells with the numerical solution obtained by the coupled finite element/boundary element method using NASHUA.[5] The specific problem solved had the characteristics listed in Table 1. The angle of incidence was chosen because several interesting features of the multiple scattering interaction are revealed in this case. For this problem, there was no internal fluid.

Table 1. Characteristics of sample problem.

$a = 1$ m	shell mean radius
$h = 0.03$ m	shell thickness
$E = 2.068 \times 10^{11}$ Pa	Young's modulus
$\nu = 0.3$	Poisson's ratio
$\rho_s = 7668.71$ kg/m^3	shell density
$\eta = 0$	shell loss factor
$\rho = 1000$ kg/m^3	fluid density
$c = 1524$ m/s	fluid sound speed
$\alpha = 0$	angle of incidence
$d = 4.0$ m	center-to-center shell separation

A finite element model of the two spherical shells was prepared using 90 low-order axisymmetric conical shell elements for each shell. Since, in axisymmetric analysis, only the generator is modeled, this mesh corresponds to a circumferential grid spacing of 2°. The resulting model had a total of 182 grid rings and 546 independent structural degrees of freedom. All structural rings were in contact with the fluid. In the fluid boundary element model, the system matrices for the fluid matrices were also augmented by the addition of 16 additional constraint equations associated with interior "Chief" points to ensure uniqueness of the Helmholtz integral representation at the upper frequencies.[22]

The non-dimensional frequency range $0 < ka = \Omega < 20$ was swept using a frequency increment of about $\Delta\Omega = 0.02$ for both the finite element and series solutions. The comparisons between the computed and exact solutions are presented in Figs. 3 and 4, which plot the (far-field) back-scattered form function [Eq. (3.30) for $\theta = \pi$ and $\phi = 0$] versus non-dimensional frequency Ω for incidence angle $\alpha = 0$ and non-dimensional center-to-center shell separation $D = 4$. Both logarithmic (Fig. 3) and linear (Fig. 4) ordinates are shown. The dashed line in the plots corresponds to the exact solution, and the solid line corresponds to the numerical solution. Clearly, very good (almost perfect) agreement is observed. The plots begin to diverge slightly only at the high frequency end.

The good agreement between the two sets of predictions serves to validate both the analytical derivation and the computational procedure. The series solution can thus be added to the short list of benchmark problems which can be used to validate large-scale structural acoustics computer programs. We note that, although the particular problem solved is structurally simple, the numerical procedure (NASHUA) is quite general, since it allows all the generality in structural modeling that CSA/NASTRAN allows.

We also note that the displayed plots are for the region below the coincidence frequency, which in this case, and for one shell, occurs at $\Omega_c \approx 38$. For shells that are very close to each other, and at low values of Ω, there is an amplitude amplification of the form function which is due to the shell-to-shell interaction effect. As the frequency Ω increases, the front

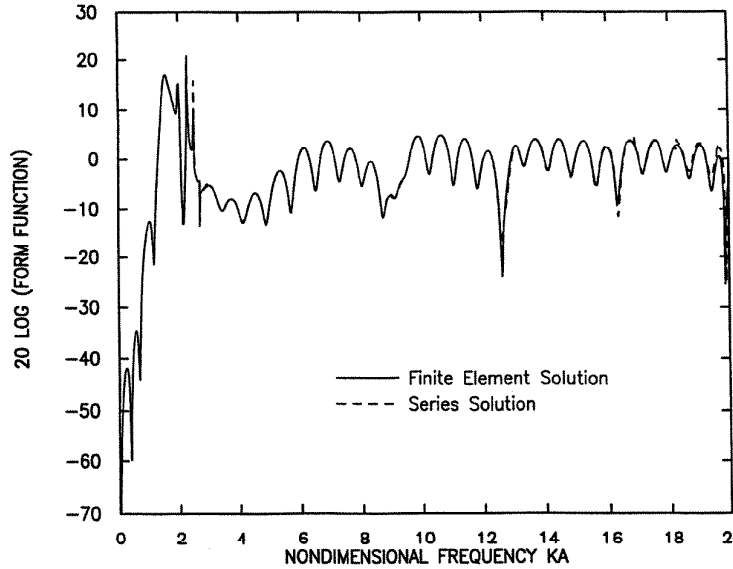

Fig. 3. Comparison between the exact (analytic) solution and numerical solution using finite elements and boundary elements. Dashed line: Exact (series) solution. Solid line: Numerical solution. This comparison is for identical shells at endfire (i.e. $\alpha = 0$) incidence. Logarithmic ordinates, dB, and $0 < ka = \Omega < 20$, and $D = 4$.

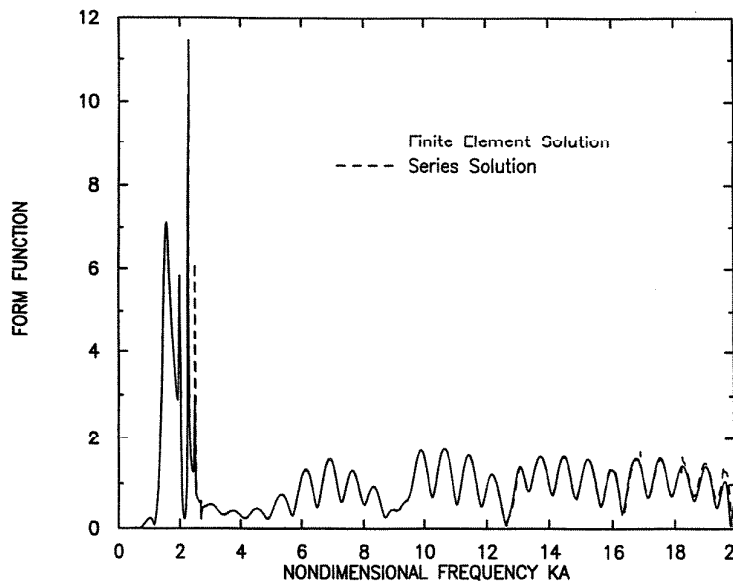

Fig. 4. Same comparison as in Fig. 3 for endfire incidence ($\alpha = 0$). The ordinates are in a linear scale, and $0 < ka = \Omega < 20$.

shell starts to eclipse the back one. For extremely high values of Ω, the presence of the back shell will no longer be noticeable in this head-on situation. As the shell separation D increases, the shell-to-shell interaction diminishes. In brief, for both amplification and eclipsing of the back shell to occur, the distance D between the shell centers must be small. The amplification of the form function could occur above the coincidence frequency due to the mid-frequency amplification effect. For the frequency range displayed in the figures, Ω is not large enough to show the mid frequency amplification effect.

Acknowledgment

The authors GCE and GCG gratefully acknowledge the partial support of the Inter-Laboratory Independent Research program at the Naval Surface Warfare Center, Carderock Division.

References

1. H. Huang and G. C. Gaunaurd, "Acoustic scattering of a plane wave by two spherical elastic shells," *J. Acoust. Soc. Am.* **98** (1995), 2149–2156.
2. L. H. Chen and D. G. Schweikert, "Sound radiation from an arbitrary body," *J. Acoust. Soc. Am.* **35**(10) (1963), 1626–1632.
3. D. T. Wilton, "Acoustic radiation and scattering from elastic structures," *Int. J. Num. Meth. Engrg.* **13** (1978), 123–138.
4. I. C. Mathews, "Numerical techniques for three-dimensional steady-state fluid-structure interaction," *J. Acoust. Soc. Am.* **79** (1986), 1317–1325.
5. G. C. Everstine and F. M. Henderson, "Coupled finite element/boundary element approach for fluid-structure interaction," *J. Acoust. Soc. Am.* **87**(5) (1990), 1938–1947.
6. M. C. Junger and D. Feit, *Sound, Structures, and Their Interaction* (The MIT Press, Cambridge, MA, second edition, 1986).
7. R. S. Cheng and F. M. Henderson, "SCATSPHERE2 — A computation for the plane-wave scattering from a submerged, elastic, spherical, evacuated or fluid-filled, thin shell," Technical Report 90/029, David Taylor Research Center, Bethesda, MD, 1990.
8. G. C. Everstine and R. S. Cheng, "Coupled BE/FE/BE approach for scattering from fluid-filled structures," In *Eighteenth NASTRAN Users' Colloquium*, volume NASA CP-3069, Washington, DC, 1990, pp. 150–164.
9. G. C. Gaunaurd, H. Huang and W. Wertman, "Acoustic scattering by elastic spherical shells that have multiple massive internal components attached by compliant mounts," *J. Acoust. Soc. Amer.* **94** (1993), 2924–2934.
10. G. C. Gaunaurd, H. Huang and W. Wertman, Response to "Comments on 'Acoustic scattering by elastic spherical shells that have multiple massive internal components attached by compliant mounts', *J. Acoust. Soc. Am.* **94** (1993), 2924–2935, and "A simple method for calculating the response from internally loaded spherical shells," *J. Acoust. Soc. Amer.* **97** (1995), 3892–3894.
11. R. Hickling, "Analysis of echoes from a hollow metallic sphere in water," *J. Acoust. Soc. Am.* **36** (1964), 1124–1137.
12. G. C. Gaunaurd and M. Werby, "Lamb and creeping waves around submerged spherical shells resonately excited by sound scattering," *J. Acoust. Soc. Am.* **82** (1987), 2021–2033.
13. H. C. Strifors and G. C. Gaunaurd, "Multipole character of the large-amplitude, low-frequency resonances in the sonar echoes of submerged spherical shells," *Int. J. Solids and Structures* **29** (1992), 121–130.

14. Y. Ivanov, *Diffraction of Electromagnetic Waves by Two Bodies*, NASA Tech. Translation F-57. National Aeronautics and Space Administration (1970).
15. A. Edmonds, *Angular Momentum in Quantum Mechanics* (Princeton Univ. Press, Princeton, NJ, 1957).
16. G. C. Gaunaurd and H. Huang, "Sound scattering by a spherical object near a hard flat bottom," *IEEE Trans. Ultrasonics, Ferroelec. and Freq. Control* **43** (4) (1996), 690–700.
17. A. P. Yutsis, I. Levinson and V. Vanagas, *Mathematical Apparatus of the Theory of Angular Momentum*, NASA Tech. Translation F-98. National Aeronautics and Space Administration (1962).
18. M. Abramowitz and I. Stegun, eds, *Handbook of Mathematical Functions* (US Gov. Printing Office, Washington, DC, 1964).
19. G. C. Everstine, "Treatment of static preload effects in acoustic radiation and scattering," In *Sixteenth NASTRAN Users' Colloquium*, volume NASA CP-2505, Washington, DC, 1988, pp. 138–152.
20. Computerized Structural Analysis and Research Corporation, Agoura Hills, CA. *CSA/NASTRAN User's Manual* (1994).
21. E. A. Schroeder, "A new block solver for large, full, unsymmetric, complex systems of linear algebraic equations," Technical Report 88/003, David Taylor Research Center, Bethesda, MD (1988).
22. H. A. Schenck, "Improved integral formulation for acoustic radiation problems," *J. Acoust. Soc. Am.* **44** (1968), 41–58.